

Modeling magnetic field in Mercury's magnetosheath

David Parunakian¹, Sergey Dyadechkin², Igor Alexeev¹, Elena Belenkaya¹, Maxim Khodachenko³, Esa Kallio² and Markku Alho²

[1] Moscow State University [Russia]

[2] Aalto University [Finland]

[3] Space Research Institute in Graz [Austria]

The general idea

- Compute magnetic field components in 82p and 162p resolution cubic grid nodes around Mercury using the enhanced paraboloid model of magnetosphere and magnetosheath.
- Run numerical hybrid simulation of plasma flow using this model of magnetic field around Mercury as input.

2016-04-20 EGU2016-8337

Fitting the initial model to MESSENGER data

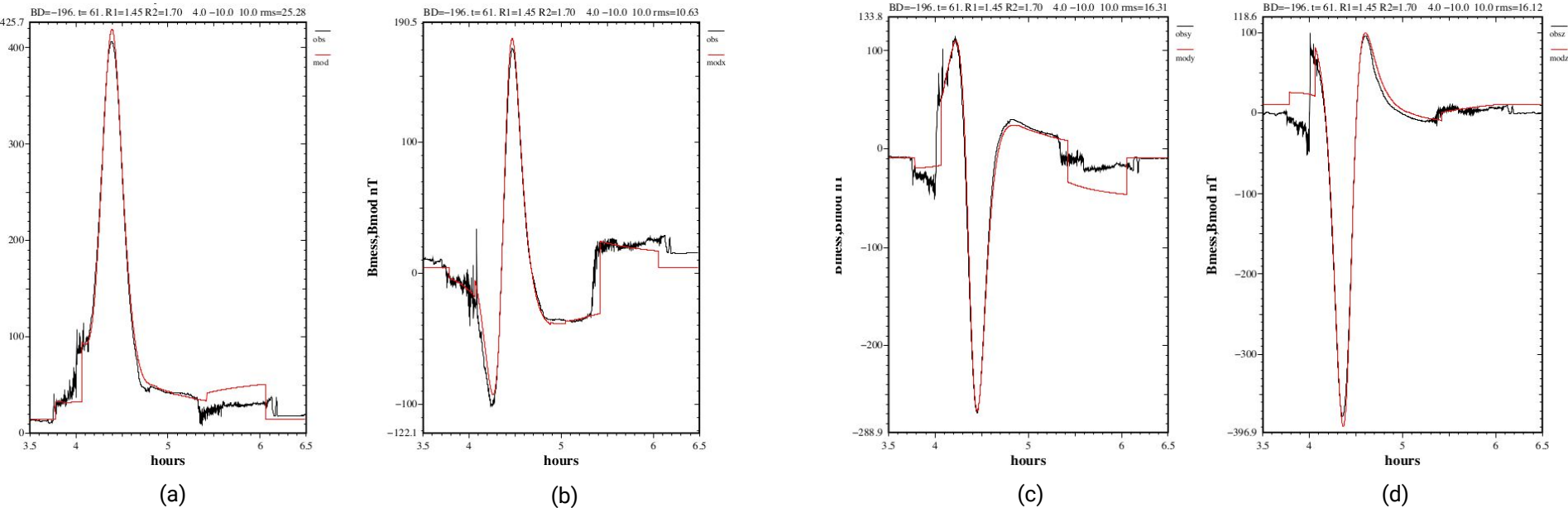


Fig.1 Comparison of **MESSENGER** data and paraboloid **model** forecast [Orbit 418] for (a) $|B|$ and (b) B_x , (c) B_y , (d) B_z field components.

Results

- The **hybrid model** produces interesting features such as **plasma depletion layer** and distinct variability between open and closed magnetospheres.
- The **enhanced PMM model** is in a good [$\sim 20\text{nT}$] agreement with MESSENGER data (especially in the bow shock region).

Next Steps

- Conduct this procedure in batch mode for MESSENGER's ~ 400 dawn-dusk magnetosphere crossings and cluster these crossings with machine learning methods [WIP].

Find out more in PICO #8337

Problem overview

1. Create a batch system for computing magnetic field in cubic grid nodes for further hybrid simulations.
2. Select dawn-dusk bow shock crossings from the available database of circa 4000 orbits.
3. Extract orbit segments inside the bow shock plus short intervals in the IMF.
4. Fit MAG data with the enhanced PMM model; use PMM parameters to calculate field in the simulation cubic grid.
5. Run hybrid simulation to estimate magnetic field and plasma density using field components initialized by enhanced PMM values.
6. Compare magnetic field along MESSENGER trajectory produced by the hybrid against MAG measurements.

Overview of Mercury

- Highly eccentric orbit (distance to the Sun 0.3-0.4 AU)
- Southwards-oriented dipole field with an estimated $196 \text{ nT} \cdot R_M^3$ magnetic moment [Alexeev et al. 2010], or less than 1% of geomagnetic field.
- Average magnetopause distance $\sim 1.45R_M$, bow shock distance $\sim 2.0R_M$ (in the subsolar point).

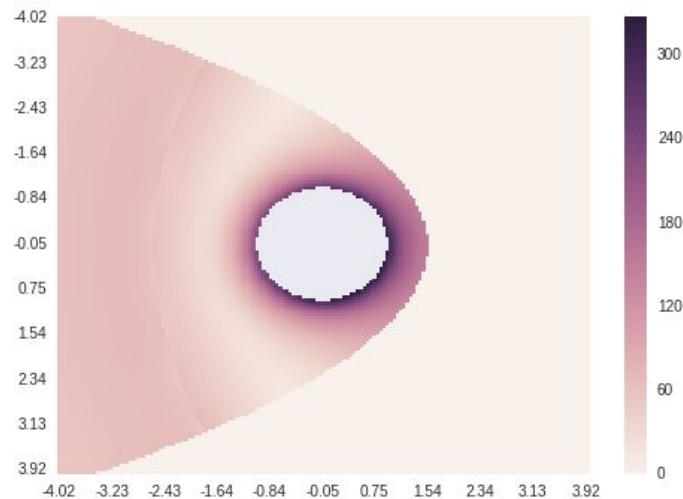


Fig.2 Mercury's magnetic field in the equatorial XY section as computed by the enhanced PMM model

Overview of MESSENGER orbit

- Inserted in Mercury's orbit in March 2011; mission ended in April 2015.
- A total of 17 orbit correction maneuvers (OCM) conducted, but only one of them drastically changed orbital parameters.

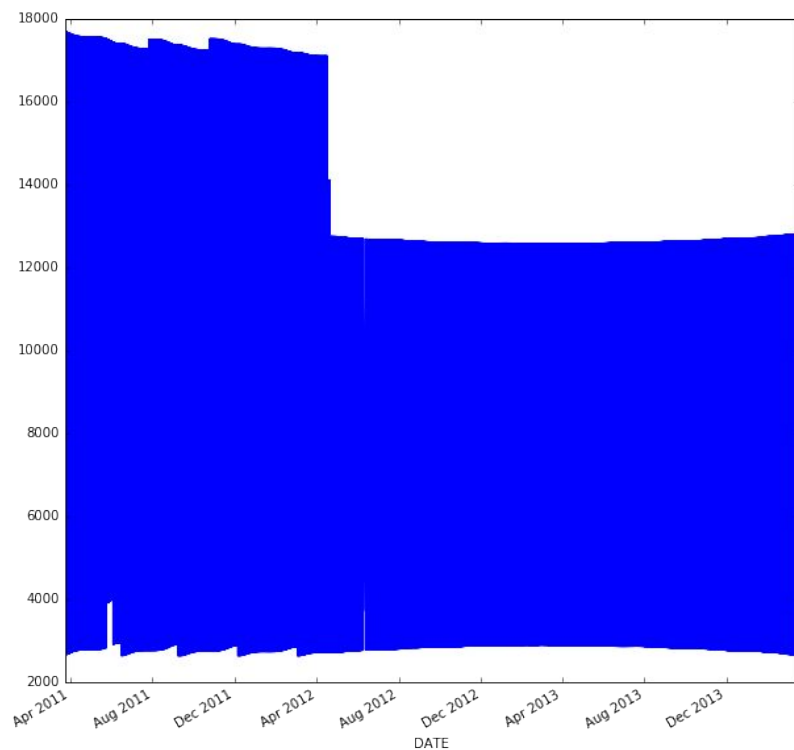


Fig.4 Variation of MESSENGER distance to Mercury during the examined dataset and sample geometry of spacecraft position.

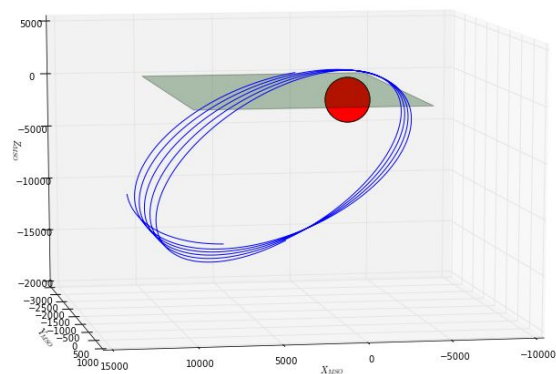
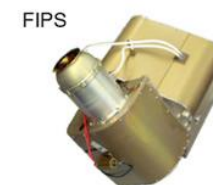


Fig.3. A slice of MESSENGER orbit

Overview of relevant MESSENGER instruments

- MAG magnetometer instrument: a three-axis, ring-core fluxgate detector high-frequency (up to 20Hz). 1/50/10/60 second averages available at ppi.pds.nasa.gov.
- Fast Imaging Plasma Spectrometer (FIPS) not fully suitable for measuring solar wind parameters due to being partially blocked by the onboard sunshade.



Dataset preprocessing: glitches

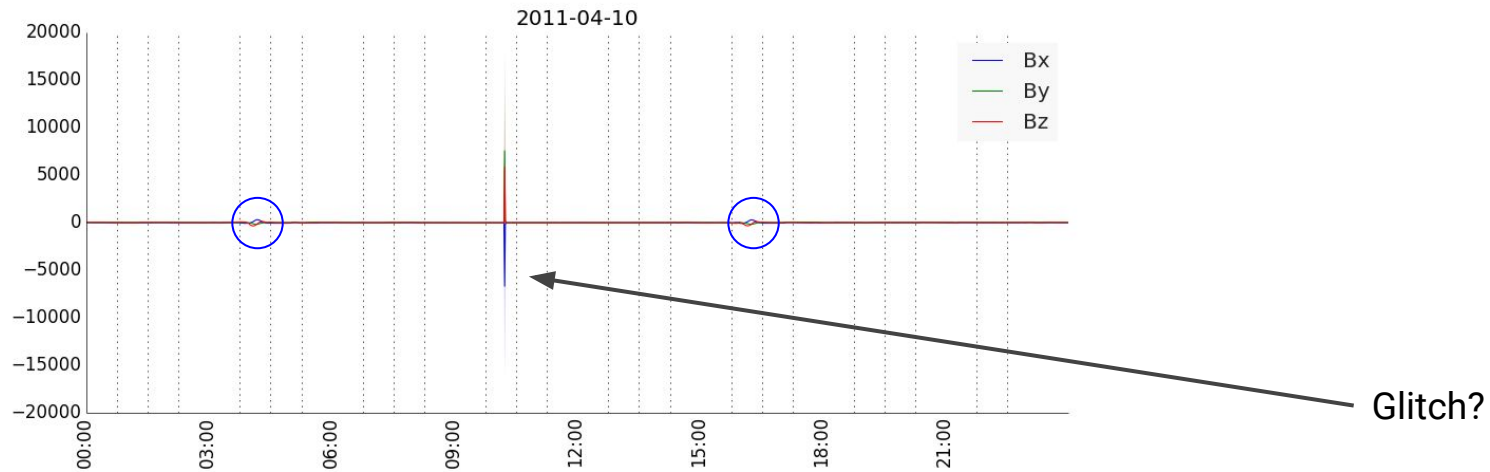


Fig 5. Example of data glitches observed in PPI MESSENGER data

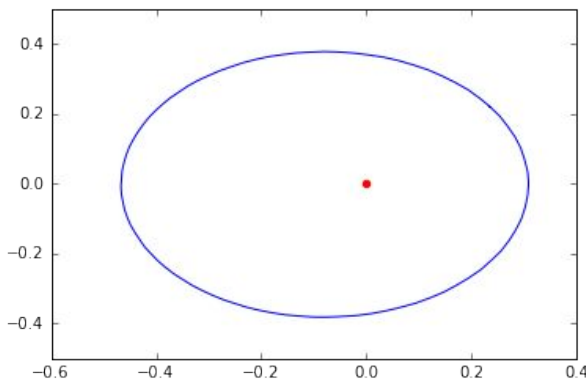
The dataset contained hundreds of data points of unknown origin corresponding to magnetic fields of several microTeslas. We believe these points to be instrument errors and remove them from our analysis.

The dataset also contained over 40 gaps in data availability. Gap lengths ranged from 2 minutes to several hours and have been treated appropriately to avoid introduction of artifacts.

Dataset preprocessing: coordinate system

- Mercury's orbital velocity varies from 40 km/s to 50 km/s along MSO Y axis depending on its position in Solar Heliographic Inertial system.
- Solar wind velocity is usually about 400 km/s.

We have to account for Mercury's motion relative to the Sun to calculate the effective direction of solar wind arrival, so next we transition to aberrated MSO' coordinate system by rotating MSO around the Z axis.

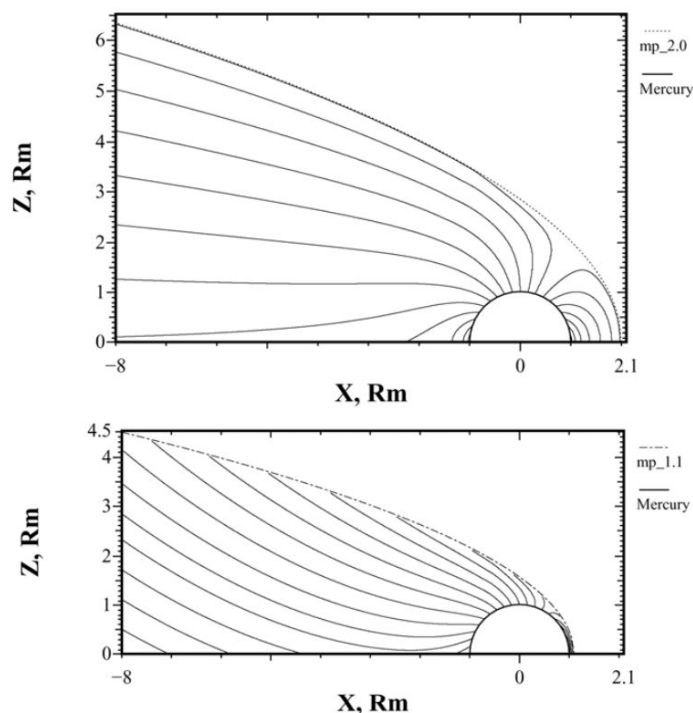


$$R_z(\theta) = \begin{bmatrix} \cos \theta & -\sin \theta & 0 \\ \sin \theta & \cos \theta & 0 \\ 0 & 0 & 1 \end{bmatrix}$$

$\theta \sim 7^\circ$

Paraboloid magnetosphere model

A paraboloidal model of Mercury's magnetospheric magnetic field based upon the earlier terrestrial model and using similar techniques. The model describes the field of Mercury's dipole which is considered to be offset from the planet's center, magnetopause currents driven by the solar wind and the tail current system including the cross-tail currents and their closure currents at the magnetopause. The effect of the interplanetary magnetic field (IMF) is modeled as a partial penetration of the IMF into the magnetosphere. [Alexeev et al, 2008]



The magnetopause is approximated as a paraboloid:

$$X/R_{sM} = 1 - (Y^2 + Z^2)/2R_{sM}^2.$$

Fig.6. Two extreme states of Mercury's magnetosphere. (a) the Hermean magnetosphere is seen to substantially expand under low SW pressure conditions (1 nPa). (b) compression of the magnetosphere by CME-like solar wind.

The hybrid model

The used hybrid simulation code is originally based on the quasi-neutral hybrid (QNH) description of plasma. Positively charged ions are explicitly treated as kinetic particles and electrons are modeled as a charge-neutralizing massless fluid. Ions and electromagnetic fields are self-consistently coupled to each other. Implicit treatment of electrons by the fluid momentum equation defines the electric field. The hybrid model platform is described in great technical detail in [Kallio and Janhunen, 2003].

Ion dynamics in the electromagnetic field is governed by the Lorentz force:

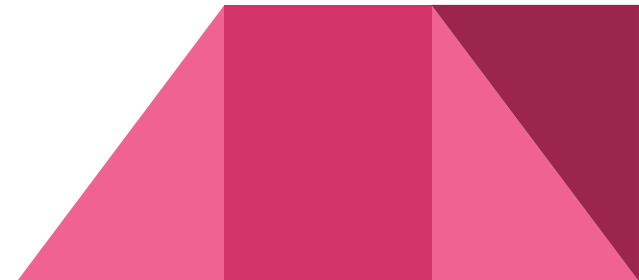
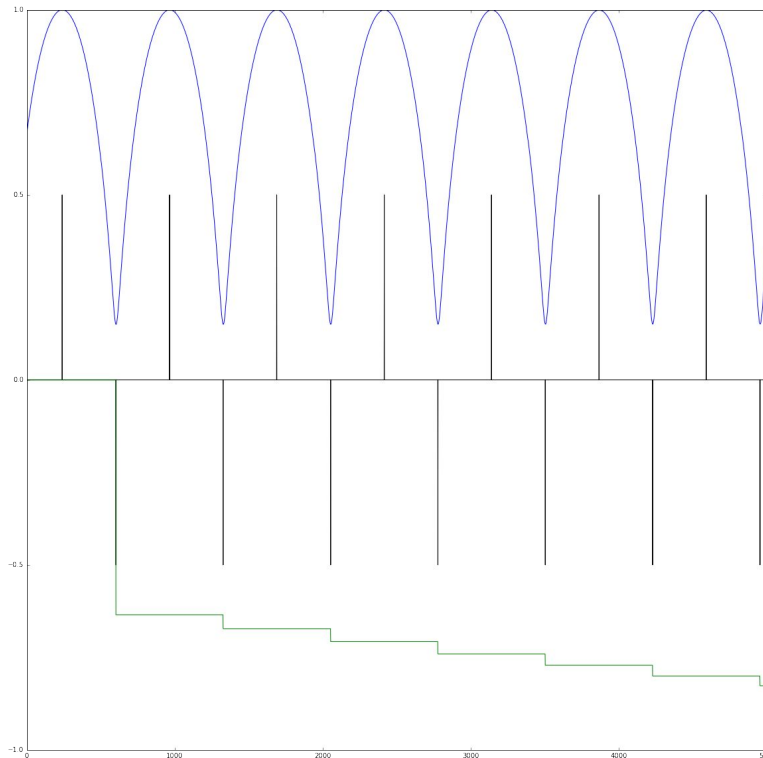
$$m_i \frac{d\mathbf{v}_i}{dt} = q_i (\mathbf{E} + \mathbf{v}_i \times \mathbf{B})$$
$$\frac{d\mathbf{x}_i}{dt} = \mathbf{v}_i$$

Electrons are implicitly represented as an inertialess fluid by the fluid momentum equation:

$$\mathbf{E} + \mathbf{U}_e \times \mathbf{B} = \eta_a \mathbf{J} + \frac{\nabla p_e}{q_e n_e}$$

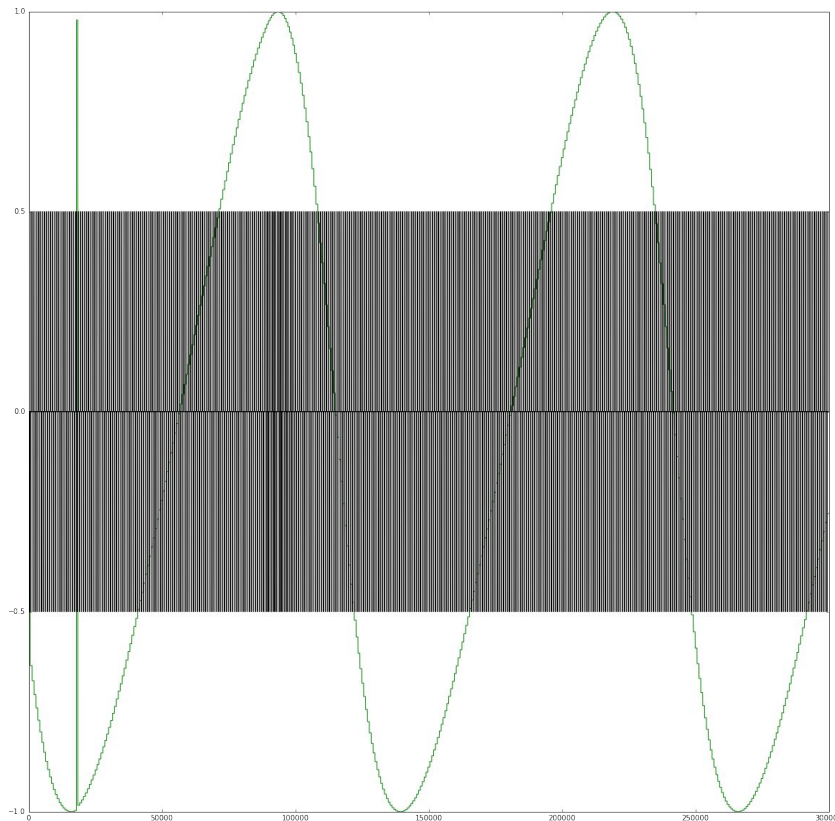
Dusk-dawn orbit selection algorithm

1. Find local ρ (X^2+Y^2) minima and maxima to determine the endpoints of orbit projections onto the XY plane.
2. Compute the angle α between Y-axis and the line connecting these endpoints.

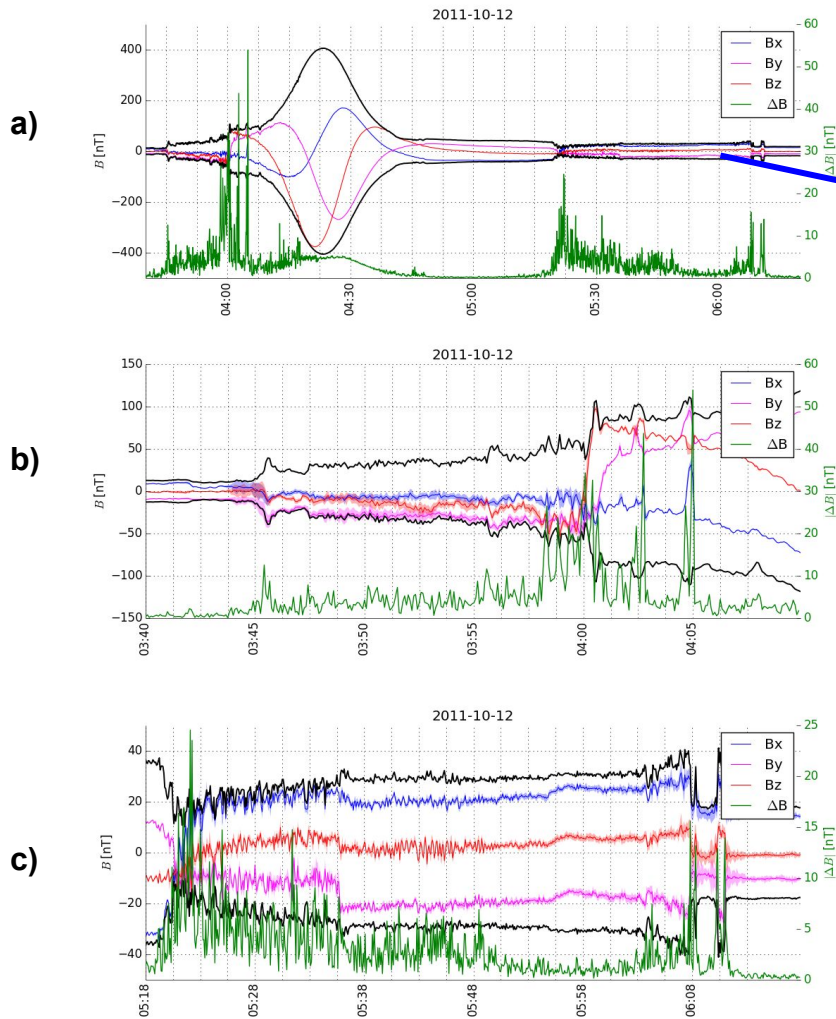


Dusk-dawn orbit selection algorithm

3. Select the orbits whose α parameter is lower than some empirically determined threshold (15 degrees in our case).



Typical magnetosphere crossing profile



d)

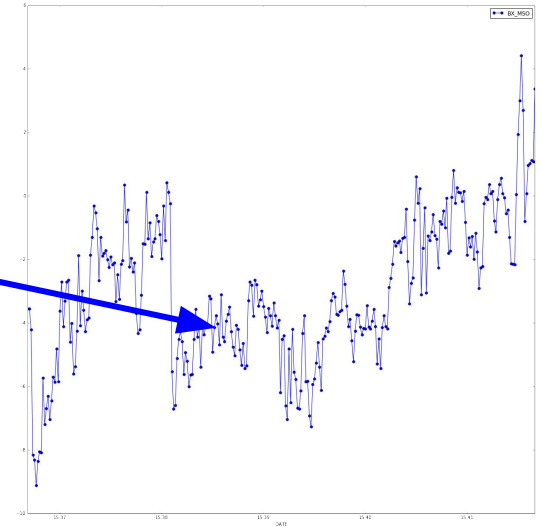
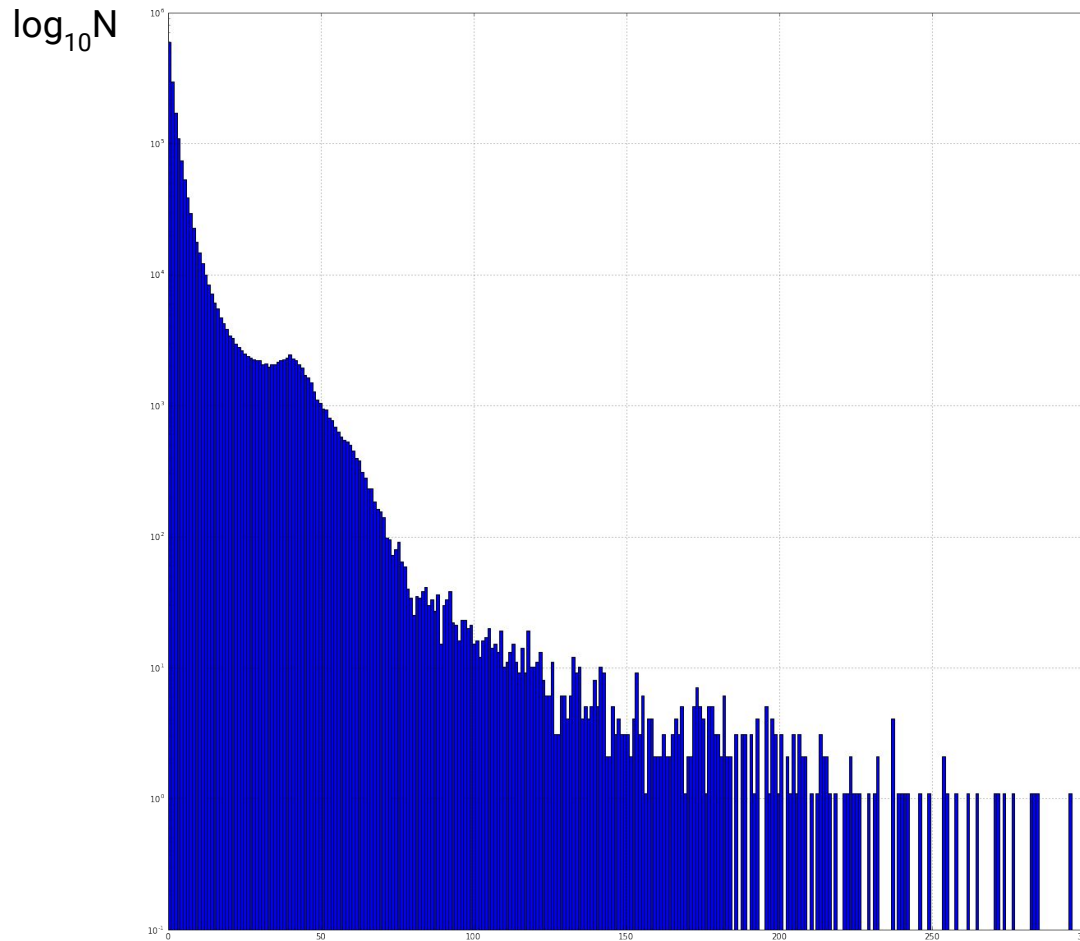


Fig.6 (a) MESSENGER Magnetometer data for the first magnetospheric transit on 12 October 2011 [Orbit 418]. Left axes give the scales for B_x (red), B_y (light green), B_z (blue), and $|B|$ and $-|B|$ (black); the right axis is the scale for B_{AC} (dark green). B_{AC} is the high-frequency magnetic fluctuations are recorded by the 1–10 Hz B_{AC} fluctuation channel. Vertical lines denote the crossing times of the inner and outer edges of the bow shock (dashed) and magnetopause (dot-dashed). (b) Close-up view of the inbound magnetosheath portion of the orbit. (c) Close-up view of the outbound magnetosheath portion of the orbit. (d) Close-up of portion of the orbit inside the magnetosheath.

Probability distribution function of $|dB_z|$



There is a clearly visible excess of fast B_z variations in the 30-50nT range. This excess probably corresponds to drastic magnetic field change on bow shock crossings, although we still need to verify this.

Fig 7. Statistical distribution of dB_z frequencies in 2011-2014 as measured by MAG

dB_z

Fitting a magnetosphere crossing with PMM

- Core paraboloid model code written in Fortran77
- BASH wrapper available for easier CGI/CLI usage.
- C-extension for Python available.
- We use Imfit library to perform fitting.
- Levenberg-Marquardt converges better than Nelder-Mead.
- To fix local minima we run the fitting procedure multiple times.

Next steps

- Run fitting procedure for all of the ~190 matching crossings
- Initialize parameters with adjacent crossing parameter values to evaluate minimization smoothness.
- Subtract the dipole field from orbit segments inside the magnetopause; normalize parameters and cluster crossings with k-means/k-medoids algorithms and Kohonen maps.

References

1. Alexeev, Igor I., et al. "Mercury's magnetospheric magnetic field after the first two MESSENGER flybys." *Icarus* 209.1 (2010): 23-39.
2. Kallio, E., and P. Janhunen. "Modelling the solar wind interaction with Mercury by a quasi-neutral hybrid model." *Annales Geophysicae*. Vol. 21. No. 11. 2003.
3. Dyadechkin, S., E. Kallio, and R. Jarvinen. "A new 3-D spherical hybrid model for solar wind interaction studies." *Journal of Geophysical Research: Space Physics* 118.8 (2013): 5157-5168.
4. Winslow, R. M., B. J. Anderson, C. L. Johnson, J. A. Slavin, H. Korth, M. E. Purucker, D. N. Baker, and S. C. Solomon (2013), Mercury's magnetopause and bow shock from MESSENGER Magnetometer observations, *J. Geophys. Res. Space Physics*, 118, 2213–2227, doi:10.1002/jgra.50237.
5. I. I. Alexeev, E. S. Belenkaya, S. Yu. Bobrovnikov, J. A. Slavin, and M. Sarantos. Paraboloid model of Mercury's magnetosphere. *JOURNAL OF GEOPHYSICAL RESEARCH*, VOL. 113, A12210, doi:10.1029/2008JA013368, 2008
6. H. Korth (APL), MAG REDUCED (RDR) DATA E/V/H/SW V1.0, NASA Planetary Data System, 2012.

Acknowledgements

This work is based on MAG instrument data collected by MESSENGER mission. We thank the scientific and engineering teams at NASA and John Hopkins University APL for their hard work.